Polymer 51 (2010) 3829–3835

Contents lists available at ScienceDirect

Polymer

journal homepage: www.elsevier.com/locate/polymer

Microgel/clay nanohybrids as responsive scavenger systems

Sebastian Berger [a], Rekha Singh [b], Janardhanannair D. Sudha [c], Hans-Juergen Adler [a], Andrij Pich [d,*]

[a] Technische Universität Dresden, Department of Macromolecular Chemistry, D-01062 Dresden, Germany
[b] Eindhoven University of Technology, Laboratory of Polymer Chemistry, P.O. Box 513, 5600 MB Eindhoven, The Netherlands
[c] National Institute for Interdisciplinary Science and Technology, Polymer Science Division, Regional Research Laboratory (CSIR), Trivandrum 695 019, India
[d] DWI RWTH Aachen University, Functional and Interactive Polymers, D-52056 Aachen, Germany

ARTICLE INFO

Article history:
Received 26 February 2010
Received in revised form
8 June 2010
Accepted 22 June 2010
Available online 30 June 2010

Keywords:
Microgel
Clay
Scavenger

ABSTRACT

Microgel–clay composite particles were prepared by one-step surfactant–free precipitation polymerization. Laponite nanoparticles present in the reaction mixture become encapsulated during the microgel formation process. Microgel–clay composites based on poly(*N*-vinylcaprolactam-*co*-acetoacetoxyethyl methacrylate) containing different amount of incorporated clay nanoparticles were synthesized. The clay content was varied from 2 wt% to 18 wt%. The extremely high incorporation efficiency of the clay nanoparticles into microgels was detected. The size of the hybrid microgels was decreased from 700 nm to 100 nm by increase of the clay concentration in the reaction mixture. Obtained hybrid microgels exhibit negative surface charge and excellent colloidal stability. Microgel–clay composite particles display temperature-sensitive behaviour in water. The swelling degree of the hybrid microgels decreases with increase of the clay loading. Microgel–clay composite particles exhibit temperature-controlled uptake of the cationic dye, Methylene blue, and can be used as scavenger systems in aqueous media.

1. Introduction

Aqueous colloidal microgels found useful applications in different areas such as coatings, agriculture, medicine, etc. due to their attractive properties such as defined size, porosity, chemical functionality and film-forming ability [1,2]. Most of the microgel particles operating in aqueous medium are based on poly(*N*-isopropylacrylamide) (PNIPAAm) [2], poly(*N*-vinylcaprolactam) (PVCL) [3,4] or other water-soluble polymers such as poly(acrylic acid) (PAA), poly(methacrylic acid) (PMA) or poly[2-(diethylamino) ethyl methacrylate)] (PDEA). The special interest in PNIPAAm- or PVCL-based microgels stems from their temperature-sensitivity which enables the fabrication of 'switchable' or 'stimuli responsive' materials.

Composite microgels [5] are of special interest due to their unique properties other than the general properties of microgels. This can be achieved by the introduction of different materials such as conjugated polymers, proteins [6], semiconductors, biomaterials, metals (Ag, Au, Pt and Pd) [7], metal oxides or sulphides in the form of nanoparticles into the porous microgel structure. In this way one can expect to obtain the multifunctional colloids where typical microgel features described above can be combined with the properties of the functional materials incorporated, such as conductivity, magnetic response, catalytic activity, etc. This approach can mostly open new possibilities for the application of colloidal particles in different technological systems. Polymer-inorganic hybrid particles have a wide application field. They are involved in the manufacture of cosmetics, inks and paints to improve the compatibility between the filler and binder. By selecting proper combination of materials and by employing the correct polymerization procedure it is possible to get desired combination of properties in these materials.

Clay is cheap, easily available but very useful filler material. It is widely used as reinforcing filler in polymers matrix enhancing their mechanical and thermal properties [8]. In such type of composites the chemical nature of the filler is often less important than the particle size and shape, the surface morphology, and the type of distribution within the polymeric matrix.

Some work has been done on the synthesis of nanocomposite hydrogels [9] using clay as a filler, study of their property change [10,11] and effect on drug release properties [12]. Many research groups have tried to incorporate clay in the polymeric particles by emulsion polymerization using unmodified [13] or covalently modified [14,15] clays which led to the particles with surface covered by clays. Covalently modified clay platelets (by using silane and titanate containing polymerizable moiety) were successfully

* Corresponding author.
E-mail address: pich@dwi.rwth-aachen.de (A. Pich).

0032-3861/$ – see front matter © 2010 Elsevier Ltd. All rights reserved.
doi:10.1016/j.polymer.2010.06.039

encapsulated inside latex particles via surfactant-free, starved-feed emulsion polymerization [16]. Zhang et al. [17] reported synthesis of hybrid PNIPAAm/clay colloids by encapsulation inorganic clay (hectorite) during polymerization process. Authors demonstrated that clay nanoparticles can also serve as cross-linking agent. In their work PNIPAAm/clay microgels were formed without use of chemical cross-linking agent.

In the recent study we present experimental results on preparation of microgel/clay hybrid colloids by precipitation polymerization. Our aim was to study the influence of the clay nanoparticle concentration in the reaction mixture on size, size distribution, swelling and temperature-sensitivity of the formed hybrid microgels. We demonstrate that incorporation of clay nanoparticles in the hydrophilic porous polymer particles is a straightforward route to design of multifunctional colloids that can be used as scavengers of organic molecules in aqueous media.

2. Experimental part

2.1. Materials

The clay used in this study was synthetic Laponite RD from Rockwood Additives Ltd (average size 10 nm) (U. K.). Acetoacetoxyethyl methacrylate (AAEM) and *N*-vinylcaprolactam (VCL) (Aldrich) were vacuum distilled under nitrogen. ω-Hydroxy poly(ethylene glycol) methacrylate (PEGMA, Aldrich) with average $M_w = 526$ g/mol and cross-linker *N*, *N*′-methylenebisacrylamide (BIS, Aldrich) was used as supplied without any further purification. Initiator (2,2′-azobis[N-(2-carboxyethyl)-2-methylpropionamidine]) (ACMA, Wako Pure Chemical Industries, Ltd.) and dye 3,7-bis(dimethylamino)-phenothiazin-5-ium chloride (Methylene blue, Aldrich) were used as received. Deionized water was employed as polymerization medium.

2.2. Synthesis of microgel/clay hybrids

The clay dispersion was prepared by ultrasonication of the clay solution in water (<2%) for 10 min. Appropriate amounts of AAEM (300 μL), VCL (1.877 g), and BIS (0.05 g; 2.15 mol%) were dissolved in deionized water (150 mL) and placed in the double-walled glass reactor equipped with a stirrer. The aqueous clay dispersion was also added (clay amounts varied from 0.011 g to 0.442 g). The reaction mixture was stirred for 1 h at 70 °C under continuous purging with nitrogen. Then an aqueous solution of the initiator (ACMA, 0.076 g) was added drop wise under continuous stirring. The reaction was carried out for 8 h. The polymer dispersions were freed from monomers and non-cross-linked polymers by dialysis. Microgels were dialyzed against water using a Millipore Dialysis System (cellulose membrane, MWCO 100.000). PEGMA macromonomer (0.3 mol% with respect to other monomers) was integrated in the polymerization recipe described above to enhance the colloidal stability of selected microgel samples used for the experiments with methylene blue and the formation of composite films. In the case of dye uptake we noticed microgel aggregation at temperatures above the volume phase transition. After incorporation of PEGMA into the microgel structure no aggregation was observed at temperatures above 40 °C due to sterical stabilization provided by the grafted PEG chains.

2.3. Uptake of methylene blue

An aqueous solution of the dye (2.398 mL, 1 mM) was taken in a 60 mL PP flask and made up to 15 mL by adding distilled water. The microgel (24.0 mg) or clay (4.8 mg) solutions were taken separately in glass vials and made up to 5 mL by adding distilled water. Clay was first dispersed in solution by sonication. Temperature of both solutions was set to the desired value using a thermostat. Both solutions were mixed and the time set as 0 min at that time. The dye-microgel mixture was stirred continuously during the whole experiment. 2 mL sample was taken out every 10 min for 1 h. Later, the time interval was increased to half an hour and 1 h. Each sample, immediately after taking from the dye-microgel mixture, was centrifuged for 5 min at 21,000 rpm and the supernatant was taken in a glass vessel for UV/Vis measurement. Similarly, a blank solution was prepared with only dye (without microgel). The UV/Vis spectra were measured in the wavelength range 200 nm–800 nm. The sample was 20 times diluted with water (250 μL was diluted to 5 mL) for the UV/Vis measurements.

2.4. Analytical methods

FTIR spectra were recorded using a Mattson Instruments Research Series 1 FTIR spectrometer. Dried samples were mixed with KBr and pressed to form a tablet.

UV/Vis spectra were recorded with a UV/Vis spectrometer (Perkin Elmer, Lambda 35). The analysis was done in the wavelength range $\lambda = 200$ to 800 nm.

XRD spectra of the hybrid microgels were recorded with a Siemens P5005 powder X-ray diffractometer equipped with a Cu K_α (wavelength 1.540 Å) radiation source using the Diffracplus software.

The thermogravimetrical analysis (TGA) was performed using a TGA 7 Perkin Elmer instrument (Pyris-Software Version 3.51). Before, measurement samples were dried in vacuum for ~48 h. Microgel samples were analysed at heating rate 10 °C/min in nitrogen atmosphere.

Particle size (hydrodynamic radius, R_h) and electrophoretic mobility were measured by a Zetasizer Nano-ZS (Malvern Instruments) (PCS). The samples were prepared by making very dilute solution in distilled water (1 drop of dispersion was added to 10 mL water (size measurements) or 10^{-3} M solution of KCl (electrophoretic measurements).

Measurements of particle size (radius of gyration, R_g) and particle size distribution were performed with an asymmetric Flow-Field-Flow-Fractionation system (F-FFF) (Wyatt, Eclipse with 350 μm spacer and DAWN DSP MALLS detector).

Sedimentation measurements to evaluate colloidal stability of microgels were performed with a separation analyser LUMiFuge 114 (L. U. M. GmbH, Germany). Measurements were made in glass tubes at acceleration velocities 3000 rpm at $T = 25$ °C. The slope of the sedimentation curves was used to calculate the sedimentation velocities and to get information about the colloidal stability of the samples.

SEM images were taken with a Gemini microscope DSM 289 (Carl Zeiss AG, Germany) instrument operating at 4 kV. Diluted dispersions were dried on a clean glass support in an oven at 20 °C in vacuum for 24 h. To increase the contrast and the quality of the images, the samples were coated with a thin Au layer to increase the conductivity and the image resolution.

TEM images have been made with a Hitachi HD 2000 instrument operating at 200 kV. Diluted microgel dispersions were placed onto carbon-coated copper grids and dried at room temperature.

3. Results and discussion

3.1. Synthesis of microgel/clay composites

3.1.1. Encapsulation of clay during precipitation polymerization

In this study clay nanoparticles were present in the reaction mixture during formation of the poly(*N*-vinylcaprolactam-*co*-

acetoacetoxyethyl methacrylate) (VCL/AAEM) microgel particles by precipitation polymerization. The synthesis procedure for VCL/AAEM microgels was reported in our earlier work [18]. In present study we used the anionic initiator 2,2′-azobis[*N*-(2-carboxyethyl)-2-methylpropionamidine] (ACMA) instead of the cationic initiator 2,2′-azobis(2-methylpropyonamidine) dihydrochloride (AMPA) employed in previous work. The selection of the anionic initiator was determined by the fact that microgel/clay microgels prepared with the cationic initiator coagulated during the particle nucleation step. We found that using ACMA stable colloidal dispersions can be obtained. However, by variation of the clay concentration in the aqueous phase we obtained a series of microgel samples with variable clay content and remarkable colloidal stability. After cleaning procedure, the microgel particles were analysed by thermogravimetrical analysis to detect the amount of clay in the hybrid particles.

Fig. 1a shows the experimentally determined and the predicted clay content in the hybrid microgels indicating that almost all inorganic nanoparticles were integrated into the polymer colloids. Fig. 1b presents IR-spectra of clay nanoparticles, VCL/AAEM microgel and hybrid particles with 18 wt% clay content. The IR-spectrum of the clay nanoparticles displays intensive peak near 1000 cm^{-1} related to Si–O stretching. This peak can be clearly observed in the IR-spectrum of hybrid microgel beside characteristic signals of VCL (amide C=O at 1623 cm^{-1}) and the ester group of AAEM (ester C=O at 1745 cm^{-1}). The intensity of the peak at 1000 cm^{-1} increased with increasing clay content in the microgel (data not shown).

XRD was used to determine the structure of the free and the encapsulated clay nanoparticles. The experimental results are presented in Fig. 2. In the case of laponite nanocrystals following values of the quotient of Bragg distances (d) and Bragg angles (2Θ values) were detected respectively: 25.1 Å/3.51 deg; 4.5 Å/19.6 deg; 2.5 Å/35.1 deg. For the hybrid samples a minor shift of the reflectance toward smaller angles was observed: 4.9 wt%: 27.6 Å/3.19 deg; 9.7 wt%: 30.9 Å/2.86 deg; 18.2 wt%: 30.0 Å/2.94 deg. However, no clear evidence that laponite nanocrystals in microgels are in intercalated form could be obtained.

3.1.2. Morphology of hybrid microgels

Fig. 3(a–c) shows SEM images of microgel samples in dehydrated state. Fig. 3a provides results of the microgel samples prepared without clay nanoparticles. The microgel particles exhibit disc-like morphology due to the deformation on the solid substrate upon drying. Fig. 3b and c illustrates hybrid microgels prepared at clay content 2.3 wt% and 8.8 wt% respectively. The size of the

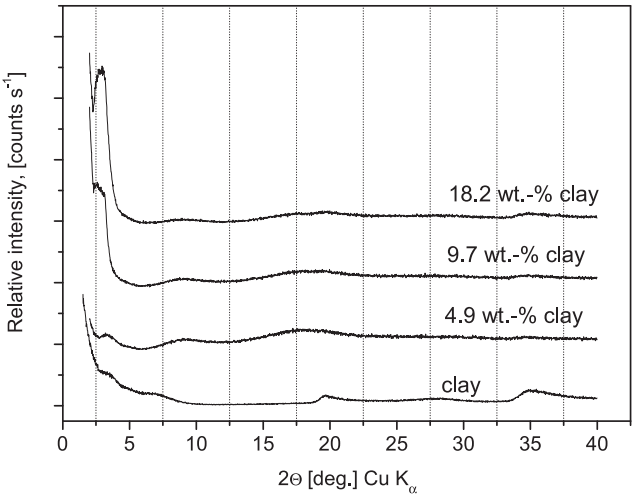

Fig. 2. XRD patterns of Laponite and composite microgels.

microgels was reduced dramatically using the clay nanoparticles during the polymerization process. The obtained hybrid microgels exhibit spherical shape and have a strong tendency to film-formation on solid substrates. We note here that particle aggregates, visible in Fig. 3b,c, are formed during the sample preparation by water evaporation. Fig. 3d shows a high-resolution TEM image of the hybrid microgels prepared at 9.7 wt% clay. The needle-like laponite nanocrystals are visible in the microgel interior (in Fig. 3d two microgel particles are shown). Clay nanoparticles are entrapped in the polymer network and do not exhibit certain orientation in the microgels.

3.1.3. Colloidal properties: size, surface charge, colloidal stability

The physico-chemical properties of the hybrid microgels were investigated using different techniques. We used asymmetric Flow-Field-Flow-Fractionation (F-FFF) coupled with multi-angle laser light scattering (MALLS) detector to investigate the size and the size distribution of the hybrid microgels. With this technique we have measured radii of gyration (R_g) for the microgel samples. Fig. 4a provides experimental F-FFF data presented in form of distribution curves (cumulative mass fraction vs. R_g) for the different microgel samples. Fig. 4a indicates that the radius of gyration of microgels decreases dramatically with increase of the clay content. At the same time the size distribution becomes narrower with increasing clay amount. The distribution curves of hydrodynamic radii (R_h) measured with photon correlation spectroscopy (PCS) presented in

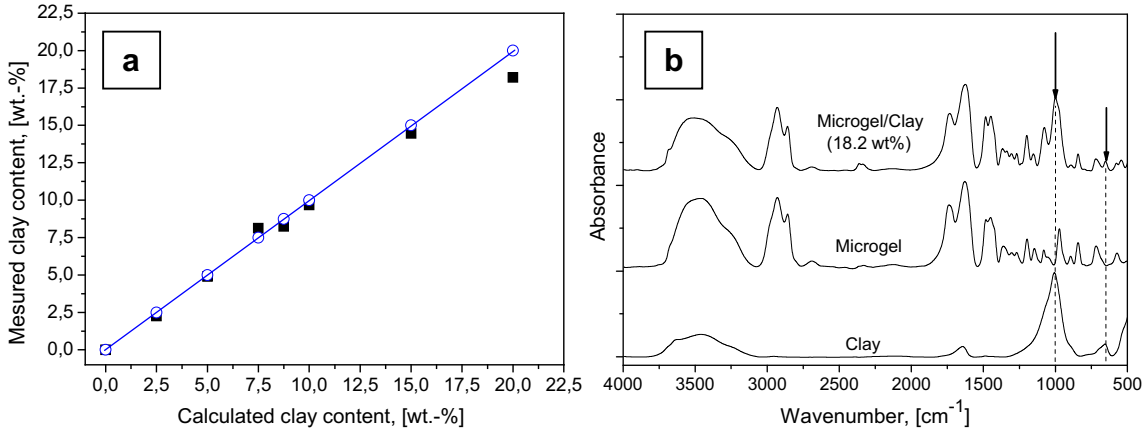

Fig. 1. Calculated (open symbols) and determined by TGA (solid symbols) clay content in the microgels (a); IR-spectra of clay, microgel and microgel/clay nanocomposites (b).

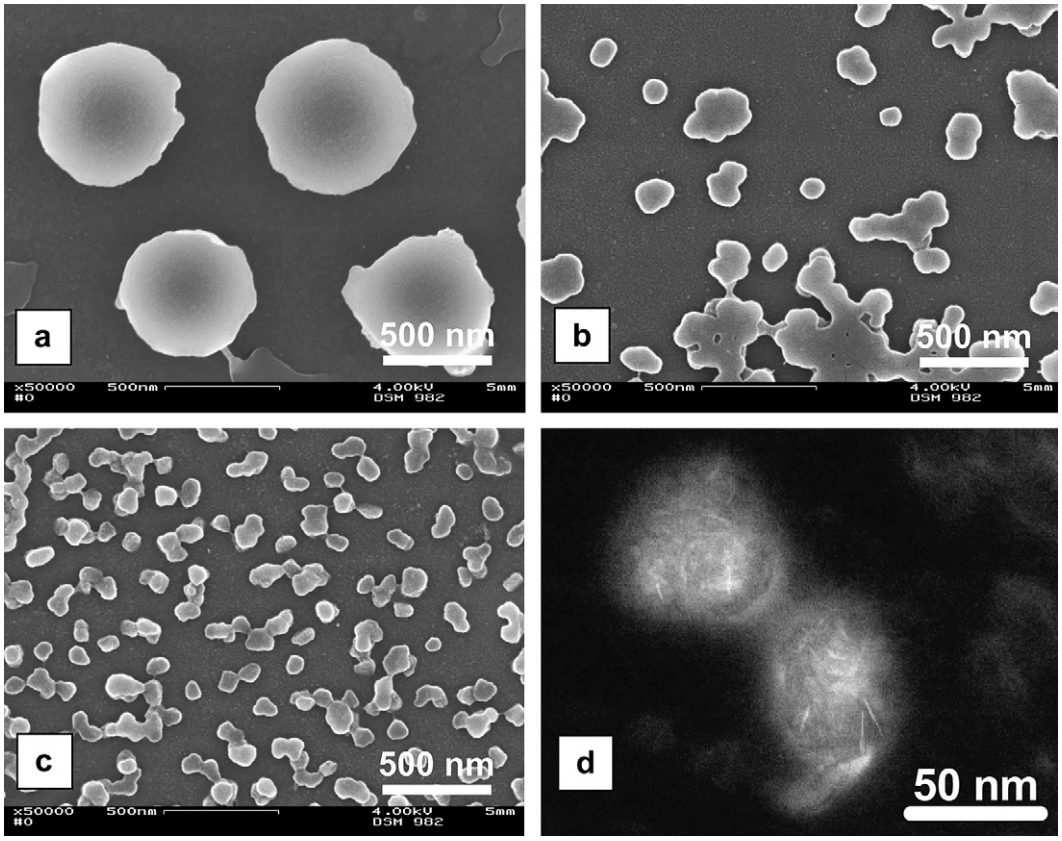

Fig. 3. SEM images of microgel particles: a) no clay; b) 2.3 wt% clay; c) 8.8 wt% clay. TEM image of microgel particles (9.7 wt% clay) (d).

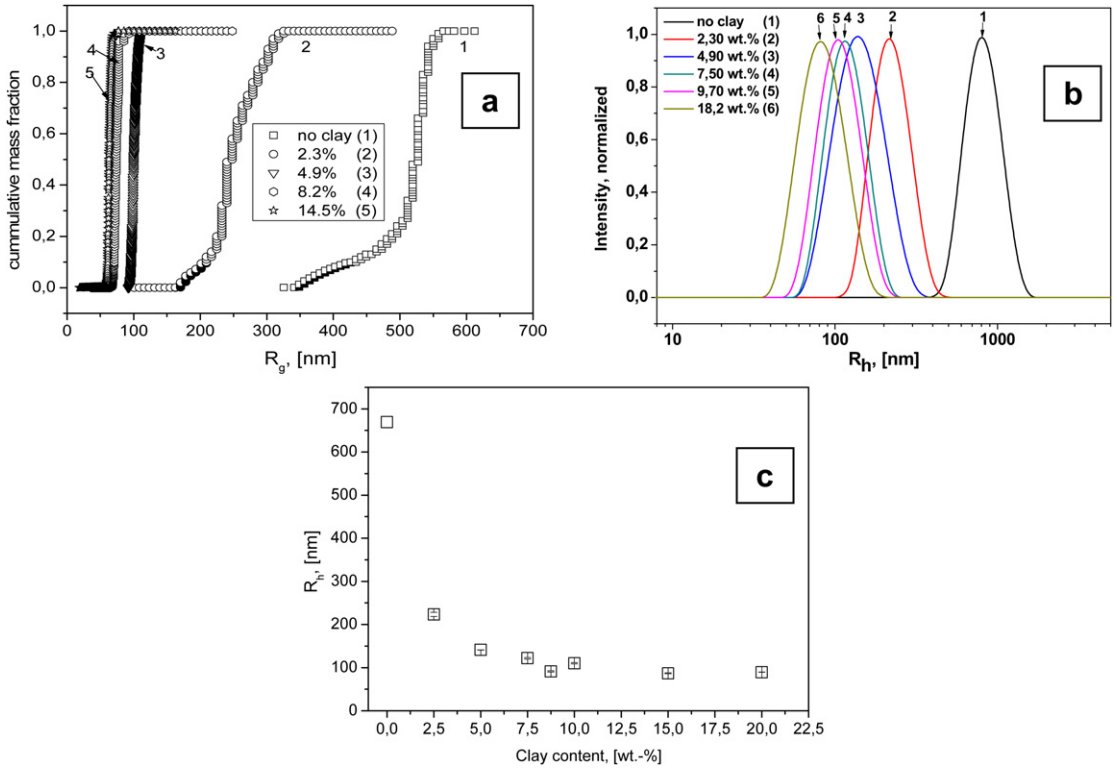

Fig. 4. Cumulative mass fraction vs. hydrodynamic radii (R_h) (F-FFF data) (a), particle size distribution curves of hydrodynamic radii (R_h) (PCS data) (b) and intensity averaged hydrodynamic particle size (PCS data) (c) for microgel samples with different clay loading.

Fig. 4b show similar trend e.g. decrease of the microgel size with increasing clay loading. The hydrodynamic radii obtained by PCS are shown in Fig. 4c as a function of the clay content in the microgels. The reduction of the microgel size and the narrowing of the size distribution in the present system can be explained by the assumption that clay nanoparticles stabilize newly formed precursor particles at the initial stages of the precipitation polymerization process. This induces the larger amount of stable precursors that do not grow by aggregation (formation of large microgels) but grow preferably by polymerization through the consumption of monomers dissolved in the aqueous phase. This leads finally to microgel particles with smaller size. Due to active participation of the clay nanoparticles in the nucleation and polymerization process they become effectively encapsulated and mechanically "locked" in the microgel network. The presence of the clay nanocrystals in the microgel interior as shown in Fig. 3d indicates that the encapsulation process takes place at early stages of the polymerization process.

We examined the surface charge and the colloidal stability of the hybrid microgels. The electrophoretic mobility data presented in Fig. 5a indicate that the clay nanoparticles exhibit negative charge in the pH range from 3 to 10. Contrary, microgel particles prepared without clay exhibit weak negative charge in the same pH range due to the ionic initiator fragments introduced during the polymerization process. For the hybrid microgels the increase of the surface charge was detected with increasing laponite content. The electrophoretic mobility data detected at pH 6 indicates a linear increase of the surface charge with increasing amount of inorganic nanoparticles in the microgels.

The colloidal stability of the hybrid microgels was investigated by a separation analyser. The sedimentation process was followed by the optical detection of the particle sedimentation front position (defined as radius from the rotor centre in Fig. 6) with centrifugation time at constant rotation speed of 3000 rpm. The sedimentation velocity data were calculated from the slope of the experimentally determined values plotted in Fig. 6. The sedimentation velocity vs. clay content in the microgels is shown as inset in Fig. 6. The sedimentation velocity decreases with increasing clay content in the microgels. Considering the high surface charge of hybrid microgels and their small size we conclude that the clay nanoparticles improve the colloidal stability of the microgels and prevent their aggregation or precipitation.

3.1.4. Temperature-sensitive properties of hybrid microgels

As it was reported in our previous work [18] VCL/AAEM microgels exhibit temperature-sensitive properties. VCL forms hydrogen bonds with water molecules through the carbonyl groups. At the same time the methylene groups of the VCL ring induce hydrophobic structuring of the water and this leads to entropy-controlled polymer–polymer interactions. If the solvent–polymer interactions are stronger than the polymer–polymer interactions PVCL chains exhibit a random-coil structure. If the hydrogen bonds to water break (due to temperature increase) the release of the structured water takes place and polymer–polymer interactions become dominating leading to the coil–globule transition. The temperature at which the phase separation for linear polymers takes place is called the lower critical solution temperature (LCST). The microgels consisting of cross-linked PVCL chains exhibit thermo-responsive behaviour and volume phase transition temperature (VPTT) close to LCST of non-cross-linked VCL chains (app. 32 °C). PVCL-based microgels swell if the temperature is below VPTT and shrink if temperature increases above VPTT. Light scattering experiments performed at different temperatures allow tracking the change of the microgel size and calculate their swelling ratio [19]. Fig. 7 shows experimental data of light scattering experiments with the hybrid microgels.

Fig. 7a indicates that the microgel sample prepared without clay and the hybrid colloids exhibits temperature-sensitive properties. Calculated swelling ratios (Fig. 7b) show that the incorporation of clay nanoparticles in microgels induces two effects. First, the temperature-induced swelling decreases with increasing clay content in the microgels. We assume that the adsorption of the

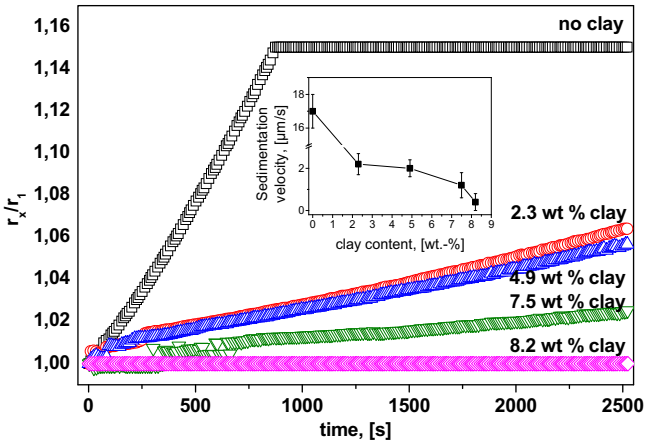

Fig. 6. Normalized position of the sedimentation front r_x/r_1 (r_x- distance from the rotor centre to sedimentation front (increases with centrifugation time); r_1- distance from the rotor centre to meniscus (constant)) as a function of the centrifugation time (inset shows calculated sedimentation velocities for the microgel with different clay loading).

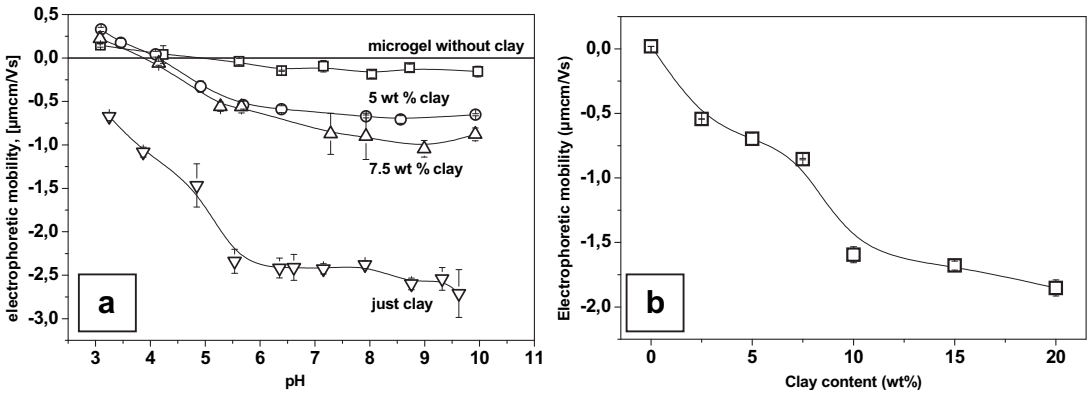

Fig. 5. Electrophoretic mobility of hybrid microgels as a function of: pH ($T = 20$ °C) (a) and clay content ($T = 20$ °C, pH 6) (b).

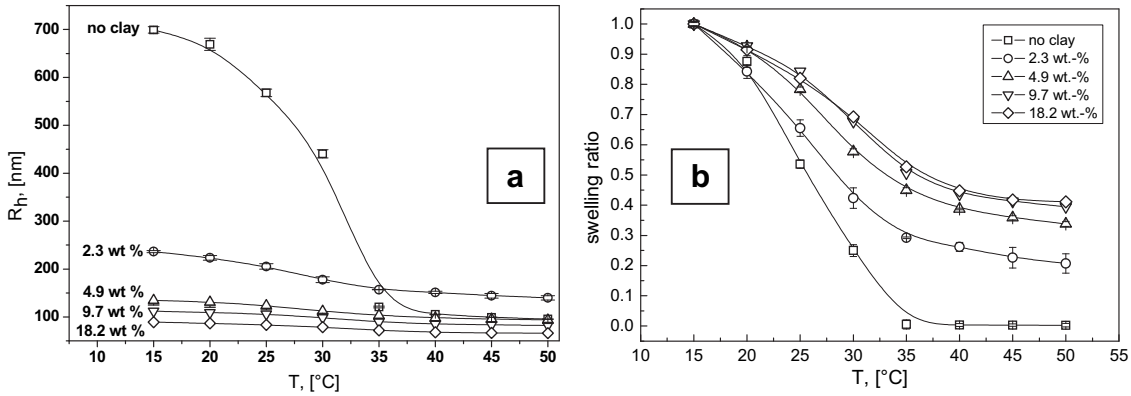

Fig. 7. Variation of the hydrodynamic radii (R_h) (a) and the swelling ratio $((R_h^M/R_h^{SW})^3$(b) with temperature (R_h^M – measured hydrodynamic radius at different temperatures; R_h^{SW} – measured hydrodynamic radius for maximally swollen microgels at $T = 15$ °C).

polymer chains on the surface of the clay nanoparticles takes place what leads to additional physical cross-linking sites. Formation of both chemical (use of cross-linker BIS) and physical (use of clay) cross-linking sites reduces the mobility of the network and reduces microgel swelling. Second, for the hybrid microgels transition region becomes broader and the particles reach de-swollen state at higher temperatures. The charged surface of laponite nanoparticles increases the electrostatic repulsion forces in the microgel network. Therefore, higher temperatures are required that hydrophobic polymer–polymer interactions start to dominate and induce the microgel shrinkage.

3.2. Microgel/clay nanocomposites as scavenger

Clay minerals have very good sorption properties for a number of water-pollutants such as dyes, pharmaceuticals or detergents [20]. Since some clay derivatives can be easily prepared and regenerated, they have been considered as promising adsorbents for environmental and purification purposes. We examined the ability of hybrid microgels to scavenge Methylene blue. Methylene blue is a heterocyclic aromatic dye which is widely used as a redox indicator in analytical chemistry and as a staining reagent in biology. This dye was already used by other groups to study its adsorption by clays [21,22].

Fig. 8a shows the UV/Vis spectrum of Methylene blue. The peak maximum around 670 nm has been attributed to the absorbance of single dye molecules, while the peak at 610 nm is attributed to a sandwich-type dimer (H-type) [23]. Fig. 8a shows the UV/Vis spectra of the dye remaining in the supernatant after 240 min extraction time with the microgels. The increase of the clay content in the microgel increases the amount of adsorbed dye molecules and reduces the dye concentration in the water phase after removing the microgels with the adsorbed dye molecules. The decrease of the peak intensities in the UV/Vis spectra of the supernatants indicates that dye molecules were removed with microgels. We assume that positively charged dye molecules are adsorbed on the clay particles via electrostatic forces.

A kinetic study of the dye uptake by microgel/clay composite particles was performed in order to follow the adsorption process. Fig. 8b indicates that more than 50% of the dye molecules adsorb immediately after adding the composite particles or the clay in the Methylene blue solution (within 5 min) followed by a slow increase in the dye uptake (the equilibrium was attained after 1–2 h for all investigated samples). For pure clay, dye uptake was found to be the highest. In the case of hybrid microgels the dye uptake increased with increasing amount of clay. For the microgel without clay, the adsorption was negligible.

The dye uptake experiments were performed at different temperatures to evaluate the influence of the sensitivity of the microgel network on the dye adsorption. Control experiments with microgels without encapsulated clay indicate that in the temperature range 10–50 °C no dye adsorption takes place. Contrary, for the hybrid microgel samples temperature can be used to regulate the dye uptake. Fig. 9 demonstrates the variation of the Methylene blue

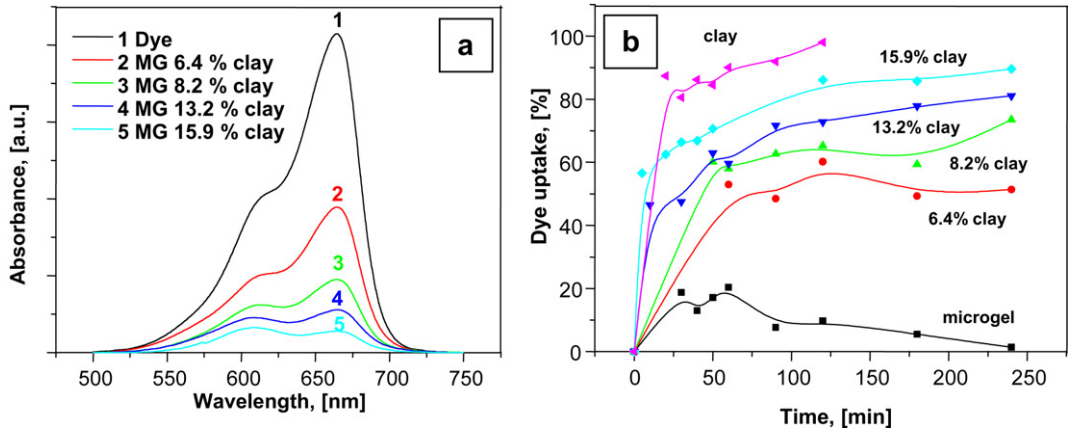

Fig. 8. UV/Vis spectra of original Methylene blue solution and solutions after extraction experiments performed with different microgel samples for 240 min (a); the uptake of the dye vs. time for the different microgel samples (b) (experimental conditions: $T = 20$ °C; microgel concentration 0.12 wt%).

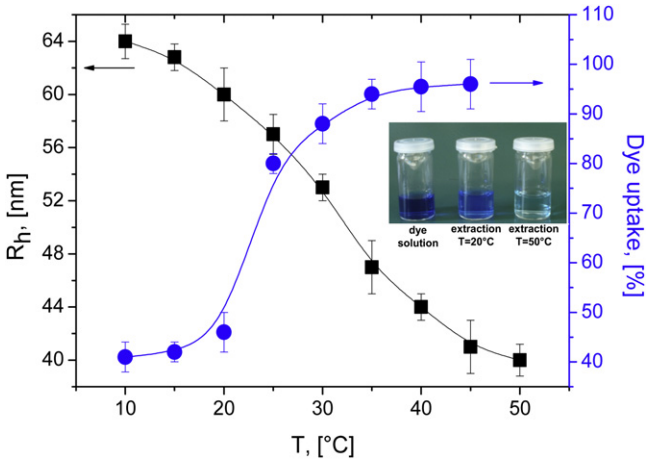

Fig. 9. Variation of the hydrodynamic radius of the microgels and the dye uptake with temperature (clay loading 15.9 wt%; microgel concentration 0.12 wt%) (inset shows photographs of the initial dye solution and dye solutions after extraction with microgels at 20 °C and 60 °C).

uptake with the temperature. As the temperature increases above VPTT of the microgel the dye adsorption is increased rapidly. The hydrophobicity of the particle interior increases during the microgel shrinkage above VPTT due to the destruction of the hydrogen bonds and the hydrophobic aggregation of the VCL units. Additionally, the shrinkage of the polymer layer around the clay nanoparticles reduces the distance of the clay nanoparticles to the microgel surface. This was confirmed by the increase of the electrophoretic mobility for hybrid microgels at temperatures above VPTT (data not shown here). We suggest that the localization of the clay nanoparticles closer to the surface of nanocomposites increases their accessibility and enhances the dye uptake.

Hybrid particles described in the present study combine attractive features of aqueous microgels (small size, porous structure, sensitivity to environment, colloidal stability) and inorganic clay nanoparticles (large surface area, reactive surface). Our preliminary results indicate that the clay nanoparticles in the microgel network can be used to scavenge organic molecules. Moreover, microgel/clay nanohybrids can be effectively used as templates for the deposition of inorganic nanoparticles (for example AgNPs) (Supporting Information, Fig. S1) or building blocks for the formation of nanostructured films (Supporting Information, Fig. S2).

4. Conclusions

Series of microgel–clay composite particles with variable clay content (from 2 to 18 wt%) were prepared by one-step surfactant–free precipitation polymerization. Laponite nanoparticles present in the reaction mixture become encapsulated during the microgel formation process. The extremely high incorporation efficiency of non-modified clay nanoparticles into the microgels was detected. The size of the hybrid microgels was decreased from 700 nm to 100 nm by increase of the clay concentration in the reaction mixture. The obtained hybrid microgels exhibit narrow size distribution and excellent colloidal stability. Incorporation of the clay nanoparticles induces the appearance of negative surface charge on the hybrid microgel surface. The microgel–clay hybrid particles display temperature-sensitive behaviour in water. The swelling degree of the hybrid microgels decreases with increasing clay loading. We suggest that the clay nanoparticles adsorb polymer chains on their surface thus providing additional physical cross-linking sites and restricting the mobility of the polymer network. The microgel–clay hybrid particles were used for the uptake of the cationic dye Methylene blue. It has been shown that the dye uptake efficiency can be tuned by temperature adjustment or by the variation of the clay loading in the microgels.

Acknowledgement

Authors thank Deutsche Forschungsgemeinschaft (DFG) and VolkswagenStiftung for financial support.

Appendix. Supplementary data

The supplementary data associated with this article can be found in the on-line version at doi:10.1016/j.polymer.2010.06.039.

References

[1] Baker WO. Ind Eng Chem 1949;41(3):511–20.
[2] Pelton R. Adv Colloid Interf Sci 2000;85:1–33;
Berndt I, Popescu C, Wortmann FJ, Richtering W. Angew Chem Int Edit 2006;45:1081–3.
[3] Peng S, Wu C. Macromol Symp 2000;159:179–86.
[4] Pich A, Teissier A, Boyko V, Lu Y, Adler H-J. Macromolecules 2006;39:7701–7.
[5] Pich A, Adler H-J. Polym Int 2007;56:291–307.
[6] Su S, Monsur ali Md, Filipe CDM, Li Y, Pelton R. Biomacromolecules 2008;9:935–8.
[7] Zhang J, Xu S, Kumacheva E. J Am Chem Soc 2004;126:7908–11.
[8] Ray SS, Okamoto M. Prog Polym Sci 2003;28:1539–641.
[9] Haraguchi K. Macromol Symp 2007;256:120–30.
[10] Haraguchi K, Li HJ. Angew Chem 2005;117:6658–62.
[11] Haraguchi K, Takehisa T. Adv Mater 2002;14:1120–4.
[12] Lee WF, Chen YC. J Appl Polym Sci 2004;91:2934–41.
[13] Cauvin S, Colver PJ, Bon SAF. Macromolecules 2005;38:7887–9.
[14] Herrera NN, Letoffe JM, Putaux JL, David L, Bourgeat-Lami E. Langmuir 2004;20:1564–71.
[15] Herrera NN, Putaux JL, Lami EB. Progr Solid State Chem 2006;34:121–37.
[16] Voorn DJ, Ming W, van Herk AM. Macromolecules 2006;39:4654–6.
[17] Zhang Q, Zha L, Ma J, Liang B. Macromol Rapid Commun 2007;28:116–20.
[18] Boyko V, Pich A, Lu Y, Richter S, Arndt K-F, Adler H-J. Polymer 2003;44(25):7821–7.
[19] Crowther HM, Vincent B. Colloid Polym Sci 1998;276(1):46–51.
[20] Ahmaruzzaman M. Adv Colloid Interface Sci 2008;143:48–67.
[21] Hajjaji M, Alami A, Bouadili AE. J Hazard Mater 2006;B135:188–92.
[22] Hang PT, Brindley GW. Clay and Clay Minerals 1970;18:203–12.
[23] Jacobs KY, Schoonheydt RA. J Coll Interface Sci 1999;220:103–11.